Mater. Res. Soc. Symp. Proc. Draft

Micromachined Lateral Force Sensors for Characterization of Microscale Surface Forces During Chemical Mechanical Polishing.

Douglas Gauthier[1], Andrew Mueller[1], Robert David White[1], Vincent Manno[1], Chris Rogers[1], Don Hooper[2], Sriram Anjur[3], Mansour Moinpour[2]

[1] Mechanical Engineering, Tufts University, Medford, MA, USA.
[2] Intel Corporation, Santa Clara, CA, USA.
[3] Cabot Microelectronics, Aurora, IL, USA.

ABSTRACT

Micromachined structures with diameters ranging from 50 - 100 μm have been applied to the measurement of the microscale shearing forces present at the wafer-pad interface during chemical mechanical polishing (CMP). The structures are 80 μm high poly-dimethyl-siloxane posts with bending stiffnesses ranging from 1.6 to 14 μN/μm. The structures were polished using a stiff, ungrooved pad and 3 wt% fumed silica slurry at relative velocities of approximately 0.5 m/s and downforces of approximately 1 psi. Observed lateral forces on the structures were on the order of 5-500 μN, and highly variable in time.

INTRODUCTION

Chemical Mechanical Planarization (CMP) is a critical process for semiconductor manufacturing. As feature sizes continue to shrink, planarity continues to be an important consideration for successful lithography. The CMP process is widely used and, for certain systems, has been characterized experimentally in terms of many of the polishing parameters. Still, a comprehensive model involving the multitude of process variables and their effects on material removal rates, planarity, and defectivity remains elusive [1,2].

The development and validation of some aspects of this "total CMP model" is hindered by lack of knowledge of *in situ* shear forces present at the micro-scale [3]. Experimental data of shear forces from single asperities would provide a comparison point for further research at this scale. In a more direct sense, knowledge of the local shear forces may be important in designing fragile structures, such as low-k dielectrics, to withstand polish.

In this paper, we detail the development of micromachined shear stress sensors intended for characterizing these *in situ* local contact forces during CMP. Other researchers have investigated the average global shear force *in situ* [4-6]. In addition, some groups have investigated micro- or nano-scale forces *ex situ* [7,8]. However, to the best of our knowledge, the work described in this paper represents the first attempt to measure local microscale polishing forces *in situ*.

DESIGN AND FABRICATION

The sensor structure is shown in Figure 1. The structures are 80 μm tall poly-dimethyl-siloxane (PDMS) cylindrical posts. The post diameters vary from 50 μm to 100 μm. Each post is recessed in a well which leaves a 50 μm wide empty region around the post. The structure is immersed into the polishing slurry and polished. As microscale features on the polishing pad come into contact with the post top, the post deflects. This deflection is observed through the back of the transparent structure using a high speed microscopy setup. Nearly 98% of the wafer surface is planar PDMS; it is only occasionally broken by the annular well region around sensor posts. This allows the majority of the normal force applied by the polishing pad to be carried by the bulk PDMS, thus not compressing or buckling the sensor posts.

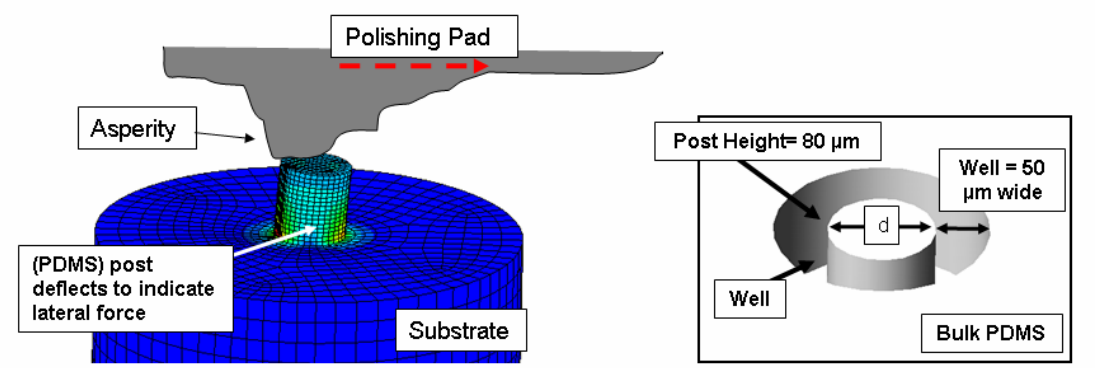

Figure 1: Diagram showing the concept of the recessed micro-post lateral force sensor.

While other researchers using micro post shear stress arrays have determined deflections optically, viewing the sensors from the top (*e.g.* [9]), this is impossible in our application due to the presence of the polishing pad. Thus, we require a transparent sensor and substrate. Our structure also avoids the need for electrical interconnects, which would be difficult to maintain and protect in a polishing environment.

PDMS is chosen because it is a transparent material with a very low elastic modulus, on the order of 750 kPa [10]. This allows deflections of 5-50 μm to be achieved with lateral forces in the range of 4-400 μN (for different diameter posts). The disadvantage of using PDMS is that it is dissimilar from the oxides and metals that are usually polished by the semiconductor industry. We emphasize that the results in this paper are for polishing of PDMS surfaces, and care must be taken when extrapolating these results to other polishing systems.

All microfabrication was conducted in the Tufts Micro and Nanofabrication Facility (TMNF). Sensors were fabricated through a modified two-layer PDMS micromolding process similar to that described in [11]. In this process a master mold consisting of two layers, one silicon dioxide and one SU-8 photoresist, is used. The silicon dioxide thin film is first lithographically patterned and etched using buffered HF to place fine features (writing and positioning marks) onto the mold. SU-8-100 (MicroChem Corp.) is then spun on at 80 μm thickness to define the main features of the structure. The master mold surfaces are silanized to aid in releasing the PDMS. Dow Corning Sylgard 184 base and curing agent is then mixed in a 10:1 ratio to produce the liquid PDMS which is degassed and poured over the mold. This is cured on a hotplate at 60 ^{o}C for 4 hours. A leveling table is used to ensure that the mold is level, creating a uniform PDMS thickness. After curing, the PDMS structure is pealed off of the mold. A microscope picture is shown in Figure 2. The compliant PDMS structure is bonded to a 0.5

mm thick Pyrex glass wafer (Corning type 7740 Pyrex glass) by exposing both surfaces to a 200 mT, 25 W oxygen plasma for 30 s, placing the PDMS and glass in contact, and heating on a hotplate at 60 ^{o}C for 15 minutes. This Pyrex wafer gives a transparent rigid backplate to the structure. A 15 nm thick Chromium film is finally sputtered onto the front side of the PDMS to aid in image contrast, and the entire structure is bonded to a stiff aluminum backing plate. The aluminum plate has windows machined in it for viewing through the backside, and includes mounting hardware for connecting to the polisher shaft.

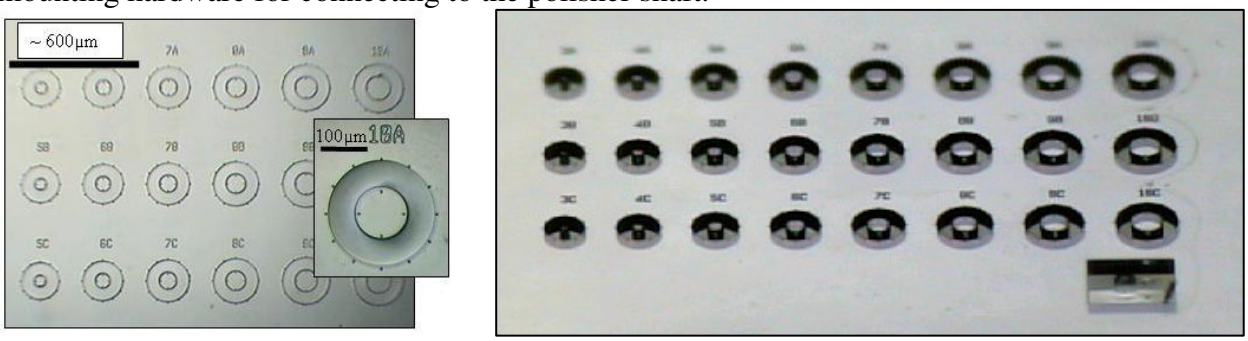

Figure 2: Light microscope pictures showing the PDMS post array. Left- perpendicular view. Right- inclined view.

CALIBRATION

Post stiffness calibration is carried out using a microscale mechanical testing technique, called MAT-Test, developed by Hopcroft *et al* [12]. The technique utilizes a contact surface profilometer to obtain force deflection curves for small structures. To determine the stiffness of the PDMS sensing posts, calibration posts (not recessed in wells) were fabricated using the same process as the experimental structures. The PDMS was cut and oriented horizontally, so that the stylus tip can travel from the base to the tip of the post. In this fashion, force vs. deflection curves are obtained for various downforces. A Veeco Dektak 6M Stylus Profilometer was used to supply downforces between 10-150 μN.

An example calibration is shown in Figure 3. The result is compared to the expected post stiffness computed using a 3D finite element model. This model uses linear elastic brick elements with a modulus of 750 kPa and a Poisson ratio of 0.5 [10]. The commercial finite element package Abaqus is used. The model includes the compliance of the base as well as the post itself, and includes geometric nonlinearities resulting from large deformations. Agreement is very good for this diameter post and for every other diameter post measured. The response is linear and fully elastic across the measured range.

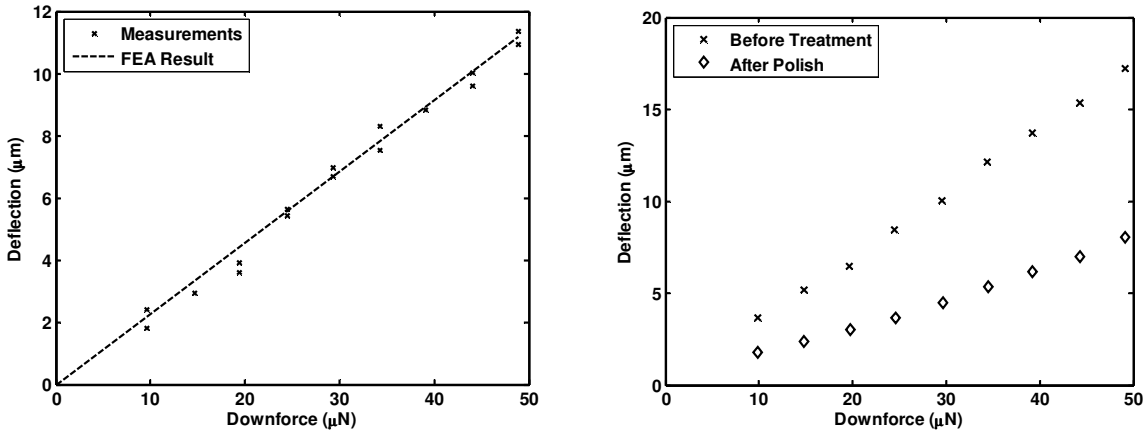

Figure 3: Post stiffness calibration examples. Left – tip lateral stiffness of a 100 μm diameter post before Oxygen plasma treatment, metallization, or polishing. Right – tip lateral stiffness of an 80 μm diameter post before and after Oxygen plasma treatment, metallization, and polishing.

Additional testing (not shown) indicated that the modulus of the PDMS is influenced by O_2 plasma treatment, aging, and polishing. The modulus increased by a factor of 3-5 after O_2 plasma treatment (used in bonding). The modulus reduced by about 10% with age (over the course of 3 days). The stiffness of one 80 μm diameter post was measured after molding (before O_2 plasma treatment or metallization) and then again after polishing, and was found to increase by a factor of 2.

The stiffness of the posts as predicted by finite element analysis and confirmed by experimental calibration prior to O_2 plasma treatment or polishing are given in the second row of Table 1. Due to the observed increase in stiffness, the stiffness used for computing lateral forces from observed deflections in situ is twice the FEA computed value, as given in row 3 of the table. It is emphasized that this has only been directly observed on a single 80 μm diameter post*, but is assumed to hold approximately true for the other size structures.

Table 1: Lateral tip bending stiffness of the micromachined posts. The stiffness before treatment was measured. The stiffness during polish is estimated based on the measurement of an 80 μm post before and after polishing (see results below).

Post Diameter (μm)	***50***	***60***	***70***	***80***	***90***	**100**
Stiffness Before Treatment (μN/μm)	0.8	1.5	2.4	3.6	5.2	7.0
Stiffness During Polish (μN/μm)	1.6	3.0	4.8	7.2*	10.	14.

RESULTS

Polishing studies were conducted in a tabletop polisher (Struers RotoPol 31) using an ungrooved IC1000 pad (Rodell, Newark, Del.). A fumed silica slurry diluted to 3% by weight particle loading (Cabot Microelectronics, Aurora, IL) was used. We emphasize again that the surface of the wafer and the sensing structures are manufactured out of the low modulus polymer polydimethylsiloxane (PDMS); this is likely to have a significant impact on the polishing forces, as compared to the polishing of stiffer materials. In addition, we emphasize that the wafer is not

rotating during these experiments due to limitations with the optical setup. The polishing pad is rotating, but the wafer is not. We are not conditioning the pad.

An optical system consisting of a Phantom v7.0 high speed camera with a 12 bit SR-CMOS sensor coupled to a 15 X relay lens and a 10 X microscope objective is used to determine post deflection during CMP. Light is provided to the sensor through the microscope objective using a fiber optic light guide and 90 degree soda lime plate beam splitter. The system is mounted on a micropositioning stage for focusing and positioning. For all experiments described here, the camera resolution and speed are set at 512 x 384 pixels and 10,000 frames per second, respectively. At 10,000 frames per second, for a relative pad speed of 0.5 m/s, asperities can be captured at 50 μm intervals. Pixel size is 2 μm. Image processing is performed on the recorded movies of post deflection to extract the relative motion of the post top. Edge detection finds points along the edge of the well and along the leading edge of the post top. Two circles are fit to these edges. The relative motion of the center of the circles gives the deflection of the post top in two dimensions. Two example images are shown in Figure 4.

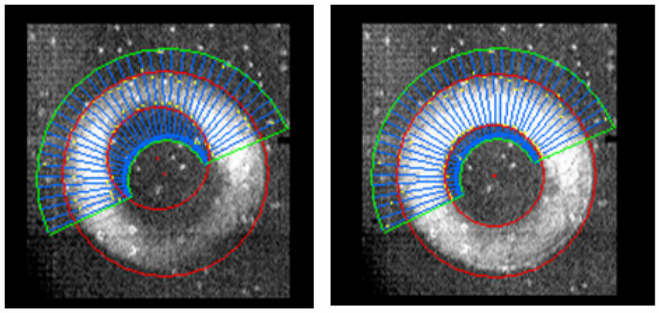

Figure 4: A post during polishing. Left – post is deflected in the direction of polish. Right – post is not deflected.

Measurements were conducted with downforces of 5 lbs, 10 lbs, and 15 lbs. This corresponds to an area average normal load of 0.4 psi, 0.8 psi, and 1.2 psi over the 4" wafer. Two different rotation speeds, 30 rpm and 60 rpm, were used for the polishing platen. The center of the wafer is approximately 10 cm from the center of rotation of the platen, hence 30 rpm corresponds to 0.3 m/s relative velocity, and 60 rpm corresponds to 0.6 m/s relative velocity. Figure 5 shows the magnitude of the maximum observed lateral forces for these various conditions on different sized structures. Increasing the size of the structure leads to an increase in lateral force. Increasing the rotation rate leads to a decrease in lateral force. An increase in downforce does not have a dramatic effect on the observed maximum lateral forces.

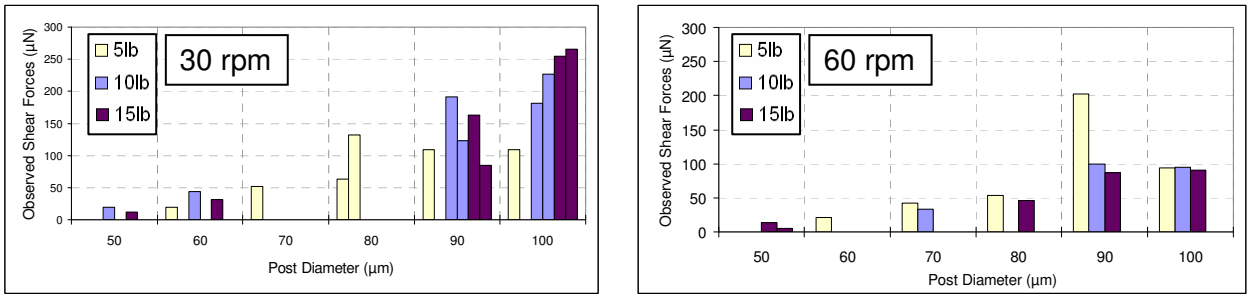

Figure 5: Summary of the *maximum* observed shear forces for a variety of conditions.

A particular time trace of the force on an individual post, along with a scatter plot showing magnitude and direction, is shown in Figure 6. The magnitude of the force is relatively low for

much of the time, but periodically spikes to higher magnitudes (above 100 μN) for brief periods of time (on the order of 1-10 ms). The direction of the large magnitude forces is usually in the direction of pad travel. Similar behavior was observed in most of the test results.

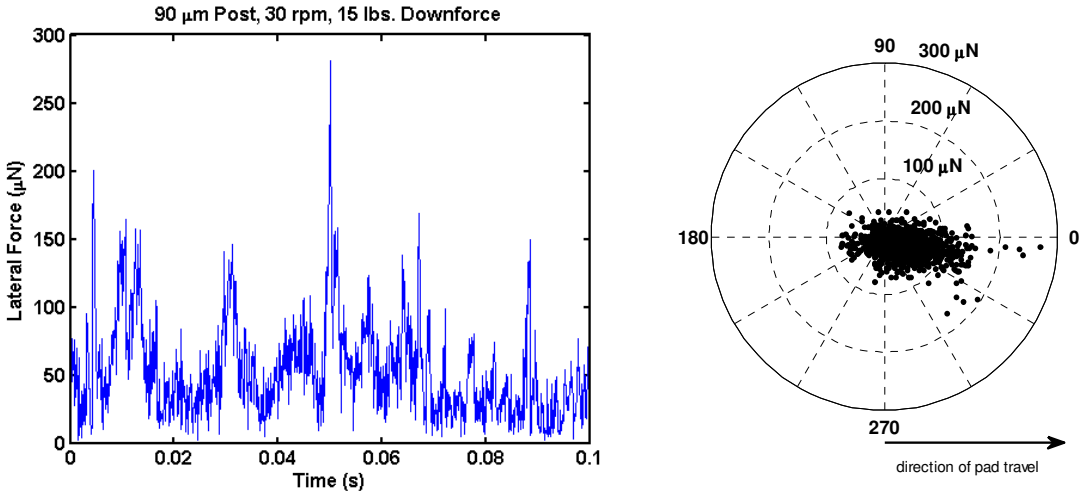

Figure 6: Example of a particular case of measured force for a 90 μm diameter post at 30 rpm (0.3 m/s) and 15 lbs. downforce (1.2 psi). Left – time history of the magnitude of the measured force. Right – scatter plot showing the magnitude and direction of the force (each point represents a single sample, taken at 10 kS/s).

DISCUSSION

The use of this sensor has provided a number of insights into the polishing forces found during CMP. It has been shown that shear forces range in magnitude from 5-500 μN. These forces scale along with increasing downforce, and they also decrease with increasing pad rotation rate. It is believed that as the rotation rate of the polishing pad increases, the polishing regime changes from one dominated by mechanical abrasion to one composed mostly of chemo/fluid interactions. It has also been shown that measured forces increase with increasing post diameter. This could be because larger diameter posts interact with multiple asperities simultaneously, thus creating larger polishing forces. Under all polishing conditions the observed forces acted primarily in the direction of pad travel, and were highly variable in time. A time trace of a single post shows that the forces are oscillatory in nature, with a period on the millisecond scale. These temporal variations in force are most likely due to asperities contacting the post and moving past at a high rate of speed.

CONCLUSIONS

During polishing of PDMS using CMP, the observed lateral forces on 50 - 100 μm diameter structures were on the order of 5-500 μN, with considerable variation of the force level in time. Larger lateral forces were observed for larger diameter structures. Increasing the speed of the polish decreased the lateral forces. Increasing the downforce increased the lateral forces at slow speeds for the largest structures, but had little impact at higher speeds. Force levels were highly variable in time, often maintaining relatively low levels on the order of 50 μN, but periodically spiking to higher magnitudes in excess of 200 μ N. This suggests that the majority of the pad and wafer are not in contact, but that large forces occur in limited regions of contact. Hence one cannot extract the local force magnitude simply from a knowledge of the global coefficient of friction.

REFERENCES

1. C. Evans, E. Paul, D. Dornfeld, D. Lucca, G. Byrne, M. Tricard, F. Klocke, O. Dambon, and B. Mullany, CIRP Annals- Manufacturing Technology, vol. 52, no. 2, pp. 611– 633, 2003.
2. E. Paul, Journal of The Electrochemical Society, vol. 148, p. G359, 2001.
3. L. Cook, Journal of Non-Crystalline Solids, vol. 120, no. 1, pp. 152–171, 1990.
4. J. Sorooshian, D. Hetherington, and A. Philipossian, Electrochemical and Solid-State Letters, vol. 7, p. G222, 2004.
5. J. Levert, F. Mess, R. Salant, S. Danyluk, and A. Baker, Tribology Transactions, vol. 41, no. 4, pp. 593–599, 1998.
6. J. Lu, C. Rogers, V. Manno, A. Philipossian, S. Anjur, and M. Moinpour, Journal of The Electrochemical Society, vol. 151, p. G241, 2004.
7. G. Basim, I. Vakarelski, and B. Moudgil, Journal of Colloid And Interface Science, vol. 263, no. 2, pp. 506–515, 2003.
8. Feiler, I. Larson, P. Jenkins, and P. Attard, Langmuir, vol. 16, no. 26, pp. 10 269–10 277, 2000.
9. O. du Roure, A. Saez, A. Buguin, R. Austin, P. Chavrier, P. Silberzan, and B. Ladoux, Proceedings of the National Academy of Sciences, vol. 102, no. 7, p. 2390, 2005.
10. D. Armani, C. Liu, and N. Aluru, Micro Electro Mechanical Systems, 1999. MEMS'99. Twelfth IEEE International Conference on, pp. 222–227, 1999.
11. S. Sia and G. Whitesides, Electrophoresis, vol. 24, no. 21, pp. 3563– 3576, 2003.
12. M. Hopcroft, T. Kramer, G. Kim, K. Takashima, Y. Higo, D. Moore, and J. Brugger, Proc. JSME Adv. Technol. Exp. Mech, pp. 735–742, 2003.